Spectral Solution of Delayed Random Walks

H. S. Bhat* and N. Kumar†
Applied Mathematics Unit, University of California, Merced, 5200 N. Lake Rd, Merced, CA 95343
(Dated: September 30, 2012)

We develop a spectral method for computing the probability density function for delayed random walks; for such problems, the method is exact to machine precision and faster than existing approaches. In conjunction with step function approximation and the weak Euler-Maruyama discretization, the spectral method can be applied to nonlinear stochastic delay differential equations (SDDE). In essence, this means approximating the SDDE by a delayed random walk, which is then solved using the spectral method. We carry out tests for a particular nonlinear SDDE that shows that this method captures the solution without the need for Monte Carlo sampling.

PACS numbers: 05.10.-a, 02.70.Hm, 05.10.Gg
Keywords: spectral method, delayed random walk, stochastic differential equations

Noise and time delays are key features of models of human balance [1, 2], circadian oscillators [3], the dynamics of gene regulation [4], cortical interneuron migration [5], and resting brain dynamics [6]. Despite the success of spectral methods in other stochastic contexts [7], delayed stochastic systems are typically not treated using spectral methods [8].

In this rapid communication, we present a spectral numerical method to calculate the probability density function (pdf) for the delayed random walk that is obtained by applying the weak Euler-Maruyama discretization to a class of stochastic delay differential equations (SDDE). We refer to the method as a spectral method because it involves solving the problem in Fourier space, and then using the inverse FFT (fast Fourier transform) to compute the solution in physical space. This method is fast, exact (to machine precision) and generalizable to other, more complicated systems.

Introduction. Consider the SDDE

$$dY_t = \phi(Y_t - Y_{t-\ell dt})dt + \gamma(Y_t - Y_{t-\ell dt})dW_t \qquad (1)$$

with initial conditions $Y(t) = \theta(t) \quad$ for $t \in [0, \ell dt]$. Here ℓ is the integer delay (lag), W_t is the standard Wiener process, and ϕ and γ are measurable functions subject to the condition that when $\gamma \equiv 0$, the resulting deterministic equation has a stable fixed point.

To obtain the pdf of a stochastic differential equation (with no delay) at time $t > 0$, a natural approach is to solve the associated Fokker-Planck equation. For an SDDE, however, the delayed Fokker-Planck equation is circular [8] and cannot be solved using standard numerical methods [8]. For this reason, past studies have applied asymptotic and perturbative methods to extract useful information from delayed Fokker-Planck equations [8, 9]. Such methods break down when the noise term is multiplied by a function of the delayed solution, or when the delay is large.

The technique employed in this paper is fundamentally different from the Fokker-Planck approach. We use a standard stochastic numerical method to discretize (1) in time and space. This discretization, together with piecewise constant approximation of the functions ϕ and γ, yields a delayed random walk approximation (4) of the original SDDE, the pdf of which is then computed using a fast and accurate spectral method.

An important reason for taking this approach is that delayed random walks can often be solved exactly [10]. Prior delayed random walk approximations to SDDE [10, 11] feature a V-shaped potential such that the walker's probabilities of right/left movements are spatially dependent. The equivalence between the Fokker-Planck equations for this delayed random walk and the original SDDE has been demonstrated [10], generalizing ideas of Ehrenfest and Kac.

Instead of using a spatially dependent potential, the delayed random walk approximation (4) allows for nonuniformity of both the sizes $K_r^{\pm}$ and probabilities $\{q_r, 1-q_r\}$ of the increments; through r, these quantities also have a piecewise constant dependence on space. This (piecewise) spatial homogeneity allows us to rewrite the system as a recursion that can be solved using spatial Fourier transforms. We view (6) as a discrete equation for the approximate time-evolution of the pdf of (1). Note that (6) differs both in derivation and solution from Fokker-Planck equations for SDDE [8, 9].

Delayed Random Walk. We discretize SDDE (1) using the weak Euler-Maruyama scheme [12] to obtain

$$Y_{n+1} = Y_n + \phi(Y_n - Y_{n-\ell})\Delta t + \gamma(Y_n - Y_{n-\ell})\sqrt{\Delta t}Z, \quad (2)$$

where Z is a Bernoulli random variable that takes values $\{-1, 1\}$ with equal probabilities. The initial conditions given after (1) yield initial conditions for (2): $Y_j = \theta(jdt)$ for $j = 0, 1, \ldots, \ell$. Let $I_{\mathcal{A}}$ denote the indicator function on the set $\mathcal{A}$. We use

$$\phi(x) \approx \sum_{r=1}^{R} \mu_r I_{[c_r, c_{r+1})}(x), \quad \gamma(x) \approx \sum_{r=1}^{R} \sigma_r I_{[c_r, c_{r+1})}(x),$$

piecewise constant approximations with constant μ_r and

* hbhat@ucmerced.edu
† nkumar4@ucmerced.edu

σ_r, and substitute back into (2) to obtain

$$Y_{n+1} = Y_n + \mu_r \Delta t + \sigma_r \sqrt{\Delta t} Z,\ c_r \le Y_n - Y_{n-\ell} < c_{r+1}. \tag{3}$$

We rewrite (3) as the delayed random walk

$$\begin{aligned} Y_{n+1} &= Y_n + K_n, \\ K_n &= K_n^r \quad \text{if} \quad c_r \le Y_n - Y_{n-\ell} < c_{r+1}, \end{aligned} \tag{4}$$

where K_n^r is a Bernoulli random variable that takes values $\{K_r^+, K_r^-\}$ with probabilities $\{q_r, 1-q_r\}$ respectively. We choose $\{K_r^+, K_r^-, q_r\}$ such that the moments of K_n^r match those of $\mu_r \Delta t + \sigma_r \sqrt{\Delta t} Z$ [13]. The delayed random walk (4) has not been considered in the literature, to the best of our knowledge. This random walk is more general than exactly solvable delayed and/or persistent random walks in the literature [14, 15].

Spectral Method. Let $\Omega = \{K_r^+, K_r^-\}_{r=1}^R$ and let α_j be the outcome of the random variable K_{n-j+1}. Applying Bayes' theorem recursively to (4), we get

$$\begin{aligned} &P(Y_{n+1} = s \cap K_n = \alpha_1 \cap \cdots \cap K_{n-\ell+1} = \alpha_\ell) \\ &= \sum_{\alpha_{\ell+1} \in \Omega} P(Y_n = s - \alpha_1 \cap K_{n-1} = \alpha_2 \cap \cdots \cap K_{n-\ell} = \alpha_{\ell+1}) \\ &\quad \times P(K_n = \alpha_1 | K_{n-1} = \alpha_2 \cap \cdots \cap K_{n-\ell} = \alpha_{\ell+1}). \end{aligned} \tag{5}$$

Denote the left-hand side as $T_s^{n+1}(\alpha_1^\ell)$ and the conditional probability as $p(\alpha_1^{\ell+1})$. Then

$$T_s^{n+1}(\alpha_1^\ell) = \sum_{\alpha_{\ell+1} \in \Omega} T_{s-\alpha_1}^n(\alpha_2^{\ell+1}) p(\alpha_1^{\ell+1}). \tag{6}$$

Taking the Fourier transform in s yields the linear system

$$\hat{T}_k^{n+1}(\alpha_1^\ell) = \sum_{\alpha_{\ell+1} \in \Omega} \hat{T}_k^n(\alpha_2^{\ell+1}) \underbrace{p(\alpha_1^{\ell+1}) e^{-i2\pi k \alpha_1}}_{M} \tag{7}$$

in k space, where $\hat{T}_k^{n+1}(\alpha_1^\ell)$ denotes the Fourier transform of the probability of reaching s by taking a sequence of steps $\alpha_\ell, \ldots, \alpha_1$ in the previous ℓ steps. In (7), we use M to denote the $(2R)^\ell \times (2R)^\ell$ matrix that gives the probability of transitioning from a sequence of states $(\alpha_{\ell+1}, \ldots, \alpha_2)$ to the sequence $(\alpha_\ell, \ldots, \alpha_1)$. Sparsity of M follows easily: since each Bernoulli random variable has only two outcomes, there are exactly two non-zero entries in every column of M for a total of $2 \times (2R)^\ell$ non-zero entries. From (7) we have $\hat{v}^{n+1} = M \hat{v}^n$, which implies $\hat{v}_n = M^{n-2\ell} \hat{v}_{2\ell}$, where $\hat{v}_n$ is a $(2R)^\ell \times 1$ vector with each component representing $\hat{T}_k^n(\alpha_\ell, \ldots, \alpha_1)$. Let $f(n,s)$ denote the pdf of the delayed random walk (4) at time step n, and let $\hat{f}(n,k)$ denote its Fourier transform with k as the variable that is Fourier conjugate to s. Then, based on the above, we have derived the solution in Fourier space:

$$\hat{f}(n,k) = \mathbf{1}^T M^{n-2\ell} \hat{v}_{2\ell}. \tag{8}$$

To compute the initial condition $\hat{v}_{2\ell}$, we require two steps. First, we use the initial condition $Y_0, \ldots, Y_\ell$ in the modified tree method (described below) to compute the exact pdf of $Y_{2\ell}$, the solution of (4) at time $n = 2\ell$. Next, we set $\hat{v}_{2\ell}$ equal to the Fourier transform in space of the pdf of $Y_{2\ell}$. In this way, the spectral method handles any initial conditions $\{Y_j\}_{0 \le j \le \ell}$ consisting of discrete random variables. This includes, for example, any set of constant initial conditions for (4), and therefore any piecewise constant initial function $\theta(t)$ for (1).

What remains is to recover $f(n,s)$ from $\hat{f}(n,k)$. Since the walk is discrete in space, $f(n,s)$ is a linear combination of Dirac delta functions,

$$f(n,s) = \sum_{m \in \mathcal{N}} f_m \delta(s - s_m), \tag{9}$$

where s_m takes specific values in s space depending on the parameters in the set Ω and $\mathcal{N} = \{-N/2, -N/2+1, \ldots, N/2-1\}$. The presence of the Dirac deltas is a reason to avoid naïve Fourier inversion of $\hat{f}(n,k)$. However, note that f is determined completely by the set $\{(f_m, s_m)\}_{m \in \mathcal{N}}$—it is this set we will solve for.

With f represented by (9), its Fourier transform is $\hat{f}(n,k) = \sum_{m \in \mathcal{N}} f_m e^{-i2\pi k s_m}$. We sample $\hat{f}(n,k)$ at discrete values of k given by $k_j = j\Delta k$ for all $j \in \mathcal{N}$:

$$\hat{f}(n,k_j) = \sum_{m \in \mathcal{N}} f_m e^{-i2\pi j \Delta k s_m}. \tag{10}$$

Let $\hat{\delta}$ denote the Kronecker delta, and assume that $\Delta k \Delta s = 1/N$. Then the inverse FFT of (10) is

$$\begin{aligned} f(n,s_r) &= \frac{1}{N} \sum_{j \in \mathcal{N}} \sum_{m \in \mathcal{N}} f_m e^{-i2\pi j \Delta k s_m} e^{i2\pi j \Delta k s_r} \\ &= \frac{1}{N} \sum_{m \in \mathcal{N}} f_m \sum_{j \in \mathcal{N}} e^{i2\pi j \Delta k (r-m) \Delta s} \\ &= \frac{1}{N} \sum_{m \in \mathcal{N}} f_m N \hat{\delta}(r-m) = f_r. \end{aligned}$$

The spectral method can now be summarized. In the first step, we compute (8), the exact solution in Fourier space, but sampled only at discrete values of k given by $k_j = j\Delta k$ for all $j \in \mathcal{N}$. In the second step, we compute the IFFT of this sampled Fourier transform at all s_m such that $m \in \mathcal{N}$. As shown, this yields the exact weight f_m corresponding to the spatial location s_m, meaning that we can indeed recover the set $\{(f_m, s_m)\}_{m \in \mathcal{N}}$ that determines (9) exactly. We denote the solution produced by the spectral method as $f_{\text{IFFT}}(n,s)$. The only source of error between $f_{\text{IFFT}}(n,s)$ and the exact pdf $f(n,s)$ is due to the inaccuracy in the IFFT algorithm itself [16].

Note that the first step requires computing the matrix-vector product n times to obtain the Fourier transform at N different points in k space, while the second step consists entirely of the IFFT. The total complexity of the spectral method is thus $N(2R)^\ell n + N \log N \sim O(n^2)$, lower than the tree-based method described below.

Choosing Δs and Δk. Since the parameters in Ω are not necessarily equal, we have a pdf over s space with

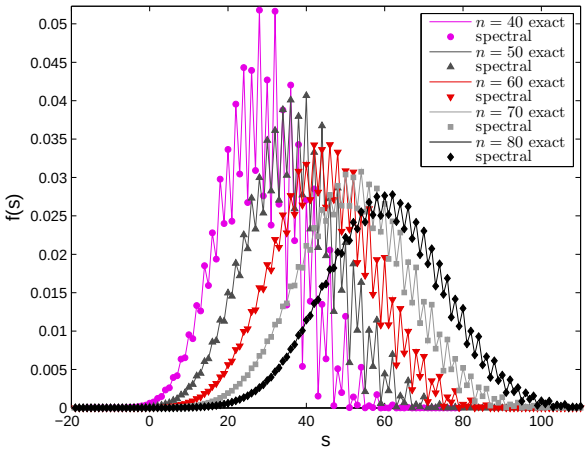

FIG. 1. Snapshots at different values of time n show machine precision agreement between the densities computed using the spectral method (each plotted with a different marker) and an enumerative exact method (each plotted using the same grayscale/color as the corresponding marker). Computed densities are for the random walk (4) with delay $\ell = 5$ and two types of Bernoulli steps K_n: outcomes $\{2, -2\}$ with probabilities $\{0.7, 0.3\}$ when $Y_n \geq Y_{n-5}$, and outcomes $\{1, -1\}$ with probabilities $\{0.9, 0.1\}$ when $Y_n < Y_{n-5}$. Initial conditions were $Y_n = 0$ for $n \leq \ell$.

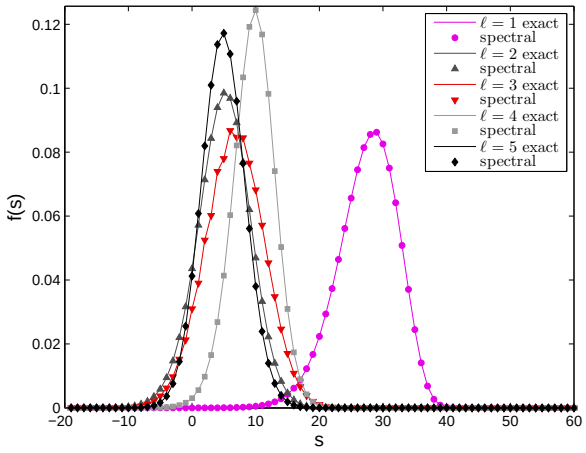

FIG. 2. For different delays ℓ, densities computed at time $n = 60$ using the spectral method (plotted using solid markers) agree to machine precision with densities computed using an enumerative exact method (plotted using lines of the same grayscales/colors as markers). Computed densities are for five different versions of the random walk (4), each with a different delay $\ell \in \{1, 2, 3, 4, 5\}$. The Bernoulli steps K_n were as follows: outcomes $\{1, -1\}$ with probabilities $\{0.3, 0.7\}$ when $Y_n \geq Y_{n-\ell}$, and outcomes $\{2, -2\}$ with probabilities $\{0.9, 0.1\}$ when $Y_n < Y_{n-\ell}$. Initial conditions were $Y_n = 0$ for $n \leq \ell$.

non-uniform spacing. We first convert this non-uniform grid into a uniform grid in order to use the IFFT. Let $\{K_r^{\pm}\}_{r=1}^R$ be rationals such that L is the least common multiple (LCM) of their denominators. Since the random walker changes its position by an element of $\{K_r^{\pm}\}_{r=1}^R$ at every step, the minimum non-zero distance between two sites that the random walker can occupy is given by $\Delta s = 1/L$. The maximum and minimum s values that can be reached by the random walker at any step n are, respectively, $S_{\max} = n \max\{K_r^{\pm}\}_{r=1}^R$ and $S_{\min} = n \min\{K_r^{\pm}\}_{r=1}^R$. This also implies that we have to calculate the pdf at $N = (S_{\max} - S_{\min})/\Delta s \sim O(nL)$ number of grid points. Since L is a constant given the parameters, we get $N \sim O(n)$, where n is the number of steps taken by the random walker. Finally, using $\Delta k \Delta s = 1/N$, we get $\Delta k = 1/(N\Delta s) = L/N$. Note that the parameters in the set Ω can be approximated such that L is small. This leads to incurring a relatively small error in calculating the pdf, while increasing the efficiency of the algorithm.

Modified Tree Method. For the delayed random walk (4), we have also developed an enumerative method for computing the exact pdf. This modified tree method involves growing a tree of all allowed paths/probabilities of the random walker. In previous work [15], the authors explained how to do this when $\ell = 1$. For $\ell > 1$, we modify the old procedure, leveraging the rationality of the increments of (4). Given the pdf at any step m consisting of $O(m)$ distinct states, computing the pdf at step $m+1$ using the tree method requires three steps: (i) calculating all possible states at step $m+1$, (ii) tracking the history and the region in which each of these states lie, and (iii) checking for recombinations to obtain the pdf at

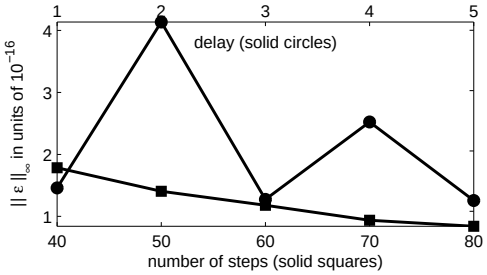

FIG. 3. Infinity norm errors $\|f_{\text{IFFT}}(n, s) - f(n, s)\|_\infty$ between the spectral and exact pdfs are at the level of machine precision, both as a function of time n and delay ℓ. Each solid square, one per value of time step n, corresponds to the $\|\cdot\|_\infty$ error between the solid markers (spectral) and lines (exact) in Fig. 1. Each solid circle, one per value of delay ℓ, corresponds to the $\|\cdot\|_\infty$ error between the solid markers (spectral) and lines (exact) in Fig. 2. All parameters are as in Fig. 1-2, respectively.

step $m+1$. Step (i) requires $2m$ operations, while (ii) requires $(2R)^\ell$ operations per state. Step (iii) requires finding unique states with the same history and summing the probabilities in each of these unique states. The overall complexity is then $\sum_{m=1}^n (2m)(2R)^\ell + m^2(2R)^\ell \sim O(n^3)$. In this work, we use this method for two purposes: to compute $\hat{v}_{2\ell}$ for (8), and to compute exact reference solutions against which we compare the spectral method.

Results. For both Fig. 1 and Fig. 2, we plot in solid lines (respectively, solid markers in the same grayscale/color) the pdf calculated by growing the tree (respectively, the spectral method). In these figures, different grayscales/colors and markers are used for different values of n and ℓ, respectively. The solid mark-

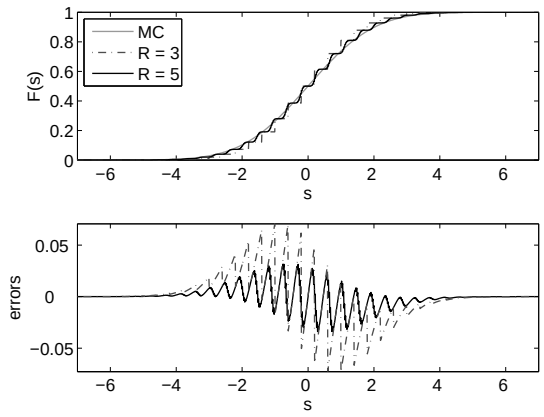

FIG. 4. For the nonlinear SDDE (11), the accuracy of the cdf computed via the spectral method increases as we increase the number of piecewise constant branches R used to approximate the tanh function. In the top pane, we plot in solid gray a fine-scale reference cdf obtained through Monte Carlo (MC) simulation with $\Delta t = 0.04$ and 10^8 sample paths. In dot-dashed gray and solid black, we plot the cdfs obtained using the spectral method with $R = 3$ and $R = 5$ approximations, respectively. In the bottom pane, we plot the pointwise errors between the spectral method cdfs and the MC cdf. The maximum error decreases from 0.0727 to 0.0337 as we go from $R = 3$ to $R = 5$. All plots are at time $t = 2$ for zero initial conditions.

ers lie exactly on the solid curves, demonstrating the accuracy of the spectral method. In Fig. 3, we plot $\|f_{\text{IFFT}}(n,s) - f(n,s)\|_\infty$ both for different numbers of steps n (in solid squares) and different delays ℓ (in solid circles). All plots confirm the spectral method's accuracy up to machine precision. To obtain the pdf at $n = 80$ in Fig. 1, the modified tree method takes 1390.8 s and the spectral method takes 0.67 s. To obtain the pdf for $\ell = 1$ in Fig. 2, the tree method from [15] takes 0.09 s, the modified tree method takes 0.29 s, and the spectral method takes 0.09 s. All simulations were done using Matlab on an 8-core Intel i7 CPU. All codes used to produce the results in the paper are available for download [17]. In all the experiments reported in Fig. 1 and Fig. 2, the spectral method is the fastest. Note that all of these results use the initial conditions $Y_j \equiv 0$ for $0 \le j \le \ell$.

Next, we apply the spectral method to the SDDE

$$dY_t = \tanh(Y_t - Y_{t-3dt})dt + dW_t, \tag{11}$$

subject to deterministic initial conditions $\theta(t) = 0$ for $t \le 3dt$. Approximating $\tanh(x)$ by $\sum_{r=1}^{R} \mu_r I_{[c_r, c_{r+1})}(x)$ and applying the weak Euler-Maruyama discretization, we get (3) with $\sigma_r = 1$ for all r, $\ell = 3$ and $Y_n = 0$ for $n \le \ell$. The error in the cumulative distribution function (cdf) calculated using the spectral method depends on the parameters R, c_r, μ_r used to approximate the tanh function; for the results shown in Fig. 4, these parameters' exact values are given in our Matlab code [17].

Setting $\Delta t = 0.04$ and $\Delta s = 0.01$ for both the $R = 3$ and $R = 5$ approximations, we compare their accuracies in Fig. 4. In the top pane, we first plot in solid gray the empirical cdf obtained at $T = 2$ ($\Delta t = 0.04$) by simulating $M = 10^8$ sample paths of the Euler-Maruyama discretization of (11)—this Monte Carlo (MC) run was performed purely to give a reference solution against which we compare the spectral method's solutions. In the same pane, we plot cdfs from spectral method simulations in dot-dashed gray ($R = 3$ approximation) and solid black ($R = 5$ approximation). In the bottom pane of Fig. 4, we plot the error between the MC cdf and the spectral method's cdfs in dot-dashed gray ($R = 3$) and solid black ($R = 5$). The maxima of the errors for the $R = 3$ and $R = 5$ approximations are, respectively, 0.0727 and 0.0337. The times taken to obtain the cdf through MC and the spectral method with $R = 3$ and $R = 5$ are 288.28 s, 0.56 s and 19.13 s, respectively. If we assume that the MC run is sufficiently fine-scale as to be close to the exact solution, these results suggest that the approximate solution will converge to the exact solution of the SDDE, as we increase R. We leave for future work a detailed discussion of convergence and optimal step function approximation.

In this rapid communication, we have developed a spectral method to obtain the pdf of a delayed random walk that is both fast and accurate. As demonstrated, this method also shows promise to solve nonlinear SDDE. In future work, we plan to extend the spectral method to solve second-order and/or oscillatory SDDE [18].

[1] T. Ohira and J. G. Milton, Phys. Rev. E **52**, 3277 (1995).

[2] J. G. Milton, J. Neural Engineering **8**, 065005 (2011).

[3] P. Smolen, D. A. Baxter, and J. H. Byrne, Biophysical Journal **83**, 2349 (2002).

[4] D. Bratsun, D. Volfson, L. S. Tsimring, and J. Hasty, PNAS **102**, 14593 (2005); K. Josic, J. M. Lopez, W. Ott, L. Shiau, and M. R. Bennett, PLoS Comput Biol **7**, e1002264 (2011).

[5] D. H. Tanaka, M. Yanagida, Y. Zhu, S. Mikami, T. Nagasawa, J.-i. Miyazaki, Y. Yanagawa, K. Obata, and F. Murakami, J Neurosci **29**, 1300 (2009).

[6] G. Deco, V. Jirsa, A. R. McIntosh, O. Sporns, and R. Ktter, PNAS **106**, 10302 (2009); G. Deco, V. Jirsa, and A. McIntosh, Nat Rev Neurosci **12**, 43 (2011).

[7] R. N. Bhattacharya and E. C. Waymire, *Stochastic Processes with Applications* (SIAM, 2009); A. Mugler, A. M. Walczak, and C. H. Wiggins, Phys. Rev. E **80**, 041921 (2009).

[8] A. Longtin, in *Complex Time-Delay Systems*, Understanding Complex Systems, Vol. 16, edited by F. M. Atay (Springer Berlin / Heidelberg, 2010) pp. 177–195; T. D. Frank, Phys. Rev. E **71**, 031106 (2005).

[9] S. Guillouzic, I. L'Heureux, and A. Longtin,

Phys. Rev. E **59**, 3970 (1999); T. D. Frank, Phys. Rev. E **72**, 011112 (2005); T. Galla, Phys. Rev. E **80**, 021909 (2009).

[10] T. Ohira and J. G. Milton, in *Delay Differential Equations*, edited by B. Balachandran, T. Kalmár-Nagy, and D. E. Gilsinn (Springer US, 2009) pp. 305–335.

[11] T. Ohira and T. Yamane, Phys. Rev. E **61**, 1247 (2000).

[12] D. J. Higham, SIAM Rev. **43**, 525 (2001).

[13] For the purposes of approximating the weak EM scheme of the SDDE, we set $K_n^r = \mu_r \Delta t + \sigma_r \sqrt{\Delta t} Z$.

[14] A. Berrones and H. Larralde, Phys. Rev. E **63**, 031109 (2001); G. H. Weiss, Phys. A **311**, 381 (2002); J. A. Rudnick and G. D. Gaspari, *Elements of the Random Walk* (Cambridge University Press, 2004); E. V. der Straeten and J. Naudts, J. Phys. A **39**, 7245 (2006); R. García-Pelayo, Phys. A **384**, 143 (2007).

[15] H. S. Bhat and N. Kumar, EJOR (2012), 10.1016/j.ejor.2012.07.003.

[16] W. L. Briggs and V. E. Henson, *The DFT* (SIAM, 1995).

[17] http://faculty.ucmerced.edu/hbhat/codes/ssdrw.tar.gz Refer to the README file for details.

[18] S. Kim, S. H. Park, and H.-B. Pyo, Phys. Rev. Lett. **82**, 1620 (1999); M. Barrio, K. Burrage, A. Leier, and T. Tian, PLoS Comput Biol **2**, e117 (2006).